Mahdi M. Hanoon
Department of Production Engineering and Metallurgy, University of Technology, Baghdad, Iraq.

Akeel A. Al-Attar
Department of Production Engineering and Metallurgy, University of Technology, Baghdad, Iraq.
attar_uot@yahoo.com

Ali M. Resen
Department of Production Engineering and Metallurgy, University of Technology, Baghdad, Iraq

The Effect of Addition of CeO_2 Nanoparticles on the Microstructure and Mechanical Properties of Ti-Al-Mg Compact Samples

Abstract-*In this research, Ti-15Al-5Mg alloy with different amount of CeO2 nanoparticles was prepared by powder metallurgy method, the powders of these materials were mixed together by ball mill then the mixed powders were pressed under high pressure, the compacted samples were sintered in electron furnace under argon gas. The density and porosity measured using Archimedes method, XRD and SEM images were used to detect phase's peaks and microstructure of all alloy sets. Vickers micro-hardness measured and Brazilian compressive tests, the results of these tests were drawing in charts with porosity and CeO2 nanoparticles percentage. From these results the best amount of CeO2 is 7 vol.% which give best mechanical and physical properties, because of created of (Ti-CeO2).*

Keywords- *Ti-15Al alloy, nanoparticles reinforcement, compact properties.*

Received on: 22/03/2017
Accepted on: 20/07/2017
Published online: 25/11/2018

How to cite this article: M.M. Hanoon, A.A. Al-Attar and A.M. Resen, "The Effect of Addition of CeO_2 Nanoparticles on The Microstructure and Mechanical Properties of Ti-Al-Mg," *Engineering and Technology Journal*, Vol. 36, Part A, No. 11, pp. 1189-1195, 2018.

1. Introduction

Titanium-aluminum-magnesium cast alloy show attractive characteristics like high strength, good hardness, kindly creep, corrosion and oxidation resistance [1]. May be because of their high stability system at elevated temperature to become softer and more durability. Increasing crack rates of fatigue are also a studied for Subugu et al. [2] Long time condition, unique properties of Ti-Al alloy had difficulty in machining processing at room temperature. But recent manufacturing methods, a good conception of the microstructure of titanium-aluminum, mechanisms of deformation, and developed of super alloys, led to the first commercial uses of titanium aluminum in a high-performance turbo for Formula One race and high speed cars [3]. Commercial techniques investigated to production of Ti-Al parts include: investment alloy and semi-liquid casting [4] and powder metallurgy method (P / M) [5]. Modern advanced methods such as mechanical alloying, laser shaping, and direct rolling have been successfully studied [6]. As many of the fast flocculation / fastening techniques such as glittering plasma sintering, discharge pulse depletion, and standardization of explosives, also succeeded in forming T-Al with the required mechanical properties [7]. While compact Ti-Al suffer from a decrease in properties, due to increased porosity and weakness phases formed during the sintering process [8]. So there are resorting to add strengthen material, these additions are working to increase the efficiency of bonding during sintering, and work on create up a strong and stable phases which increase the mechanical properties of this alloy [9].

Ceramic nanoparticles reinforcement has been widely used in various engineering applications [10]. The fabrication and characterization of nanoparticles prepared by powder technology techniques has been extensively investigated. Many types of nanoparticles, including SiC, Al_2O_3, ZrO_2, CeO_2, carbon nanotubes, and diamond, have been used to enhance the mechanical, physical, thermal, electrical, chemical or corrosion behavior of many alloys such as Ti, Al, Fe, Ni … etc. alloys [11].

Cerium oxide CeO_2 is a rare earth oxide, has attracted considerable interest in metal-matrix. Balathandan et al. [12] observed that Ti main alloys strengthened with micron and sub-micron sized CeO_2 particles displayed significant corrosion resistance related with that of Ni-ZrO_2, Ni-Al_2O_3, and high pure Ni. Li et al. [13] prepared Ni–Zn/CeO_2 composite and investigated

https://doi.org/10.30684/etj.36.11A.9
2412-0758/University of Technology-Iraq, Baghdad, Iraq

the effects of CeO_2 on the hydrogen evolution reaction activity.

This paper reports the apparent density and porosity, microstructure, micro-hardness, and Brazilian compressive of Ti-12Al-5Mg/nano-CeO2 obtained by powder technology isotactic pressure with a high apparent density.

2. Experimental work

Use of titanium powder (pure titanium) produced the company (CT-3000-SG and CT-3000-SDP Almatis, Germany) and purity 99.7% with particle size 35μm, and aluminum powder (pure aluminum) production company (TZ-3YE Tosoh, Japan) and purity 99.5% and the size of the crystals 25 μm, and magnesium powder (pure magnesium) produced the company (TZ-3YE Tosoh, Japan) and purity 99.5% the size of the crystals 53μm. The three powders are mixed with each other with different proportions of CeO_2 nanoparticle size powder 50nm as shown in the Table 1, using ball-mill as a mixing device for a period of half an hour to ensure homogeneity and volumetric chemical. Powder mixture pressure as batches the weight of each batch is 100g, when the amount of pressure 175 MPa and consistency for 5 second with using a cylindrical die from the tool-steel dimensions of (2x7 cm), after which the samples were taken out of carefully the mold. Sintering process was conducted using an electric furnace type (IDUGTO-model S17) at a temperature of 650 °C and using Argon gas to prevent oxidation during heating. Sintering process is done in two steps; the first step preheat process occurs by rise the furnace temperature up to 300 °C and the installation of 60 minutes as shown in Figure 1, this step is important for ensuring the removal of moisture before the sintering process, to reduce the contraction of the samples during sintering.

While in the second step the furnace temperature rises to 650 °C and the installation of 120 minutes, the samples are remained in the furnace until they reach room temperature, while the heating and cooling rate were 5 °C/min.

3. The Inspections and Tests

All samples were prepared by grinding process used grind SiC paper, then samples were polished using cloth pad and Al2O3 liquid as a polished liquid.

I. Apparent Density and Porosity

Apparent Density $\rho_a$and $\Gamma_a$porosity of produced porous ceramics was measured by the water immersion principle based on "Archimedes' method" according to ASTM C20-00 [14]. The procedure of immersing method is to: i) weight the dry sample, ii) weight the immersing sample in distilled water for 25 h, and iii) weight the saturating sample. The equations of apparent density ρ_a and percentage of apparent open porosity Γ_a are [15]:

$$\rho_a = \frac{W_d}{W_d - W_i} \times \rho_{H_2O} \left(g/cm^3\right)$$

Where W_d is the dried weight, W_i is the immersed weight and W_s is the saturated weight.

Apparent porosity is determined by weighting the prepared samples in air, then suspended it in a liquid and measured the soaked weight in air and used the formula:

$$\Gamma_a\% = \frac{W_s - W_d}{W_s - W_i} \times 100\%$$

II. Linear Shrinkage

The influence of temperature on longitudinal linear shrinkage is studied. In this test, sample lengths are measured before and after sintering, then getting shrinkage percentage by following shrinkage formula [16]:

$$\mathcal{S}\% = 1 - \frac{L_t}{L_o} \times 100$$

Where $\mathcal{S}\%$ the shrinkage percentage, L_t and L_o represent sample length after sintering, initial sample length respectively.

III. X-ray Diffraction and Microstructure

Crystalline phases were identified by X-ray diffraction (XRD) using a SHIMADZU X-RAY Diffractometer, XRD-600 with monochromatic CuKα radiation. The applied voltage and current were 40.0 kV and 30.0 mA, respectively. The finding is generally from 20 º to 80 º and a period size of 0.02 º with a rapidity of 1.2 º/min. The size for sample of XRD analysis was 3mm × 3mm × 3mm. The pore size and wall thickness were determined using a Hitachi S-570 SEM, and different areas were arbitrarily selected in each sintered specimen. SEM sample dimensions were 5mm × 3mm × 3mm.

IV. Micro-Hardness

Micro-hardness device model (VENDRE, FW100) was use to examine the hardness of sintered samples were extracted results on a digital screen which connected with the micro-hardness device. Examination was done for five samples of each samples set, then draw a chart was showing the effect of the added on the hardness values.

V. Brazilian Compressive Strength

The Brazilian disk test, which is a diametrical compression inspection, is used to quantity the compressive strength for all sintered samples. This test is usually used for materials that are too hard to process or machine into ASTM standard's dog-bone samples for tensile testing [17].

The compressive strength in the direction perpendicular to the freezing direction was measured using a universal testing machine. Sintered specimens were circular disks with dimensions of 10mm × 5mm. A tensile machine with a crosshead speed of 5mm/min (Instron machine/IMR) was used for compression tests.

Compressive Brazilian strength was measured using the following equation [18]:

$$\sigma_c = \frac{2P}{\pi Dt}$$

Where $\sigma_c$is the compression strength (MPa), P is the cross head load (N), D is the specimen diameter (mm), and t is the specimen thickness (mm).

4. Results and Discussion

A conclusion should point out the distinguished Figure 2 shows the apparent density is increasing with increase the amount of addition of CeO_2 nanoparticles, thus decrease the percentage of porosity, due to the small size of the granules nanoparticles that are closing the pores between the grains of mixture powders. As well as to increase the granules of powder mixture as a result of the work of the nanoparticles additive as thermal concentration centres and thus help to be contact areas between the mixture grains [8-10].

Figure 3 formed the most important phases of the samples after the sintering process, shows clearly be phases (Ti15Al-5Mg), (α-Ti) and (Ti-CeO_2). Ti-CeO_2 is a hard phase and inert chemical reactions [19] in terms of the process, and it appears to increase the severity of phase with increasing the amount added. Figure 4 shows the SEM images and the microscopic structure of the samples is noted to be the protective layer on the surface of the containing nanoparticles added samples, and noted that the thickness of this layer increases with increase of nano-added amount [15].

Micro-hardness test results are described in Figure 5, which shows that the micro-hardness increases with increase of nanoadditives quantity, the main reason for that is due to create of (Ti-CeO_2) hard and stable phase, that is deposited on the grain boundaries, so that led to increases the hardness of the alloy [17].

Compression strength for compacted samples after sintering process are increased with increasing of nanoparticles amount, it is clear in Figure 6, the reason for this increasing of compression strength values, in addition to create of (Ti-CeO_2) hard and stable phase, is to increase contact points between mixed powder grains, which leads to reduced porosity and thus increasing compressive strength of alloy [20].

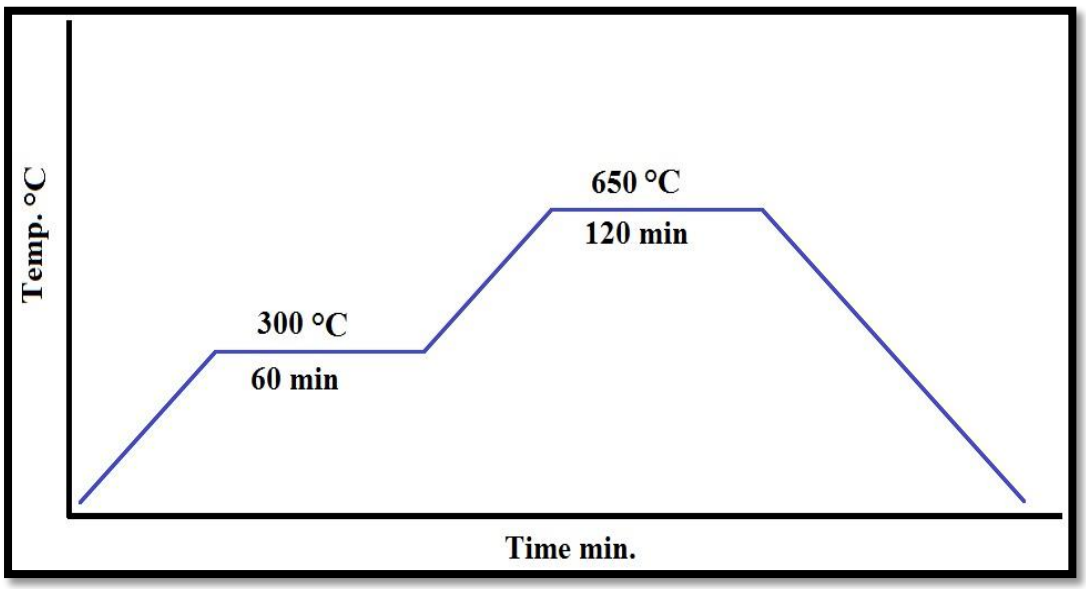

Figure 1: Heat and sintering processes applied on compacted samples.

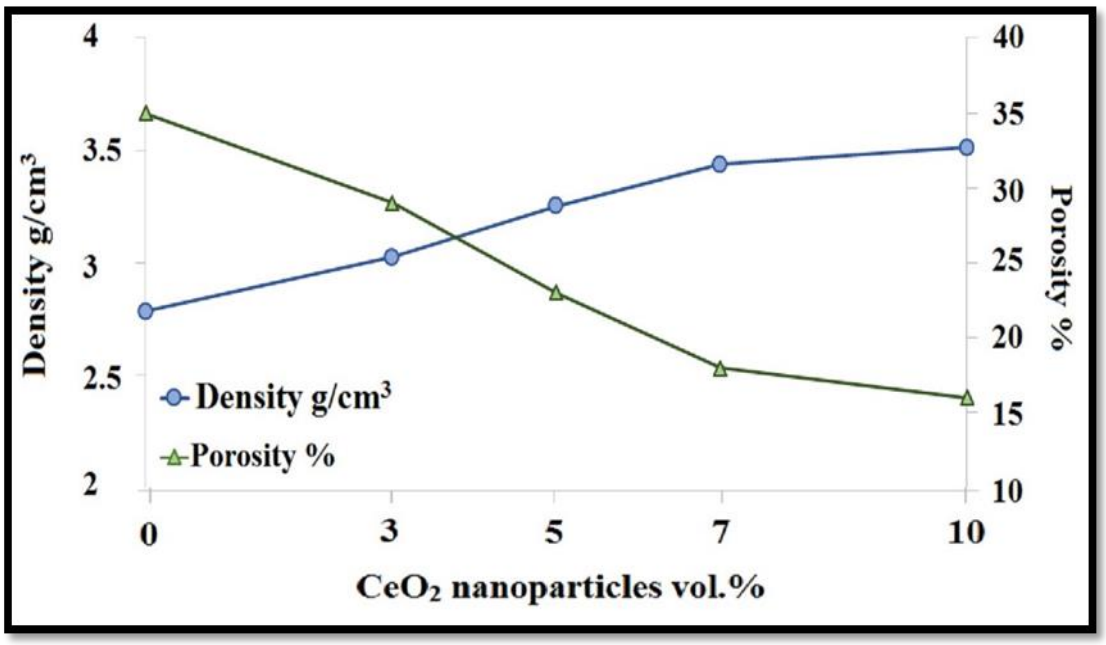

Figure 2: Effect amount of CeO2 nanoparticles on the density and porosity of Ti-15Al-5Mg alloy.

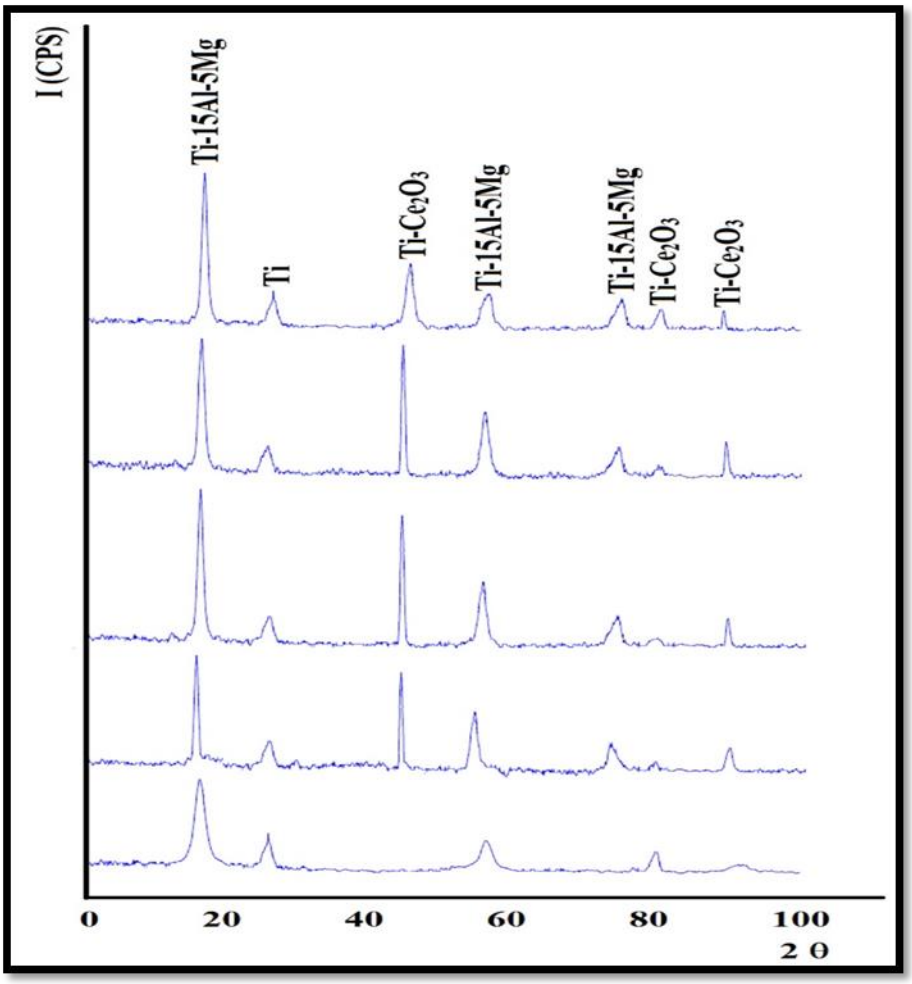

Figure 3: XRD peaks of the important phases with different amount of CeO_2 nanoparticles.

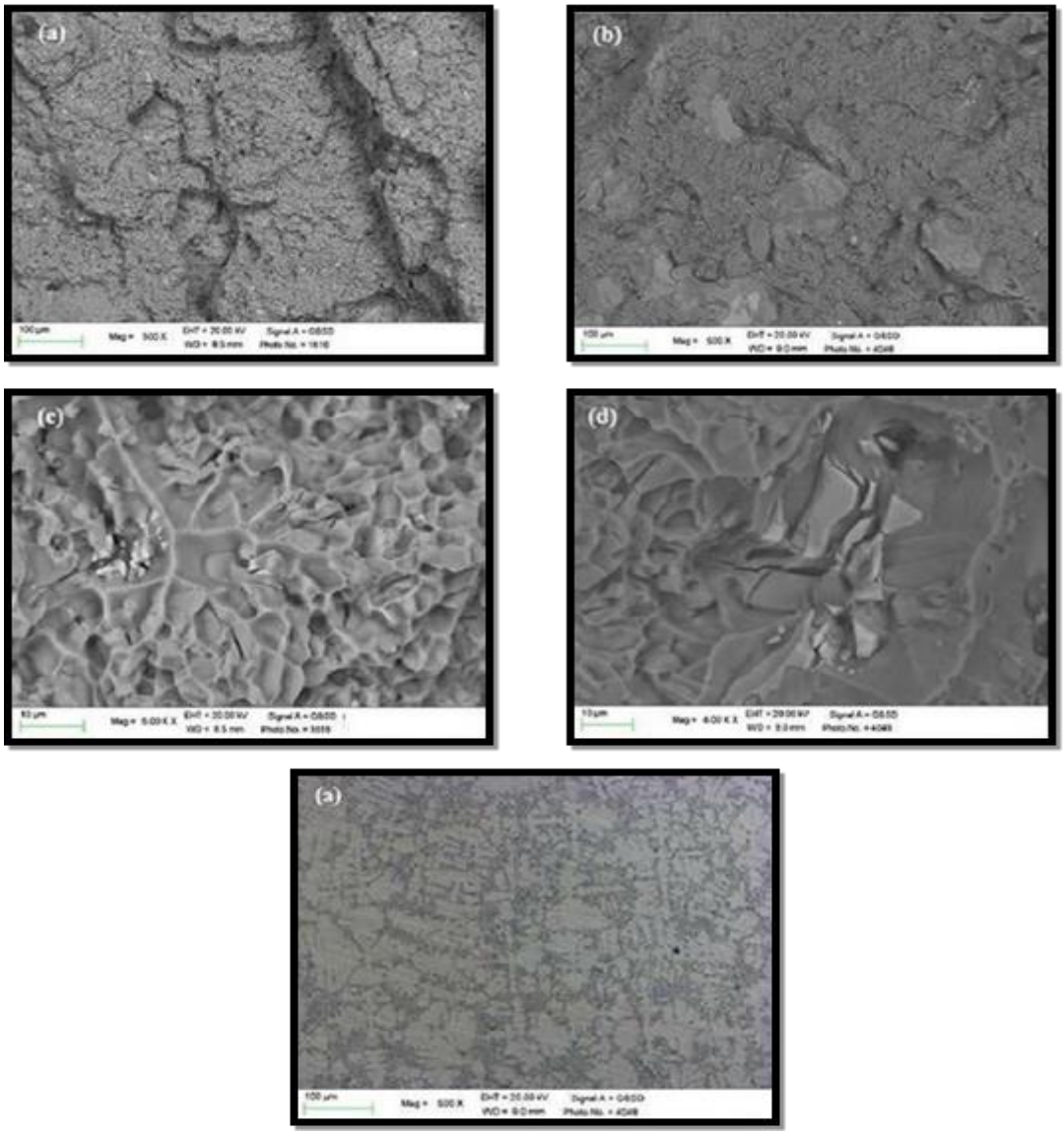

Figure 4: Microstructure of sintered samples;
a) Alloy set 2, b) alloy set 3, c) alloy set 4, d) alloy set 5, and e) alloy set 1.

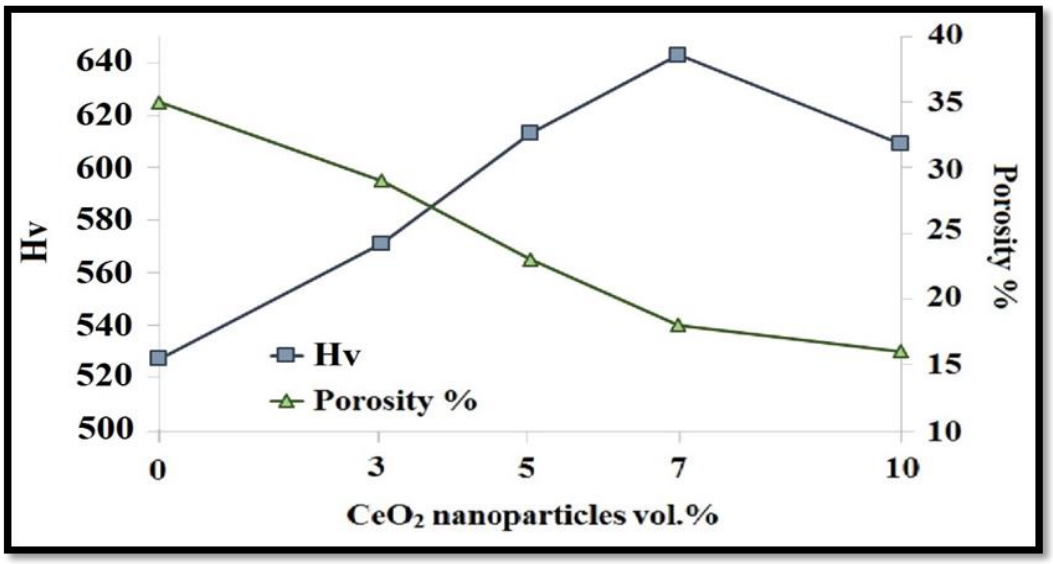

Figure 5: Effect of nanoadditives and porosity percentage on the micro-hardness values.

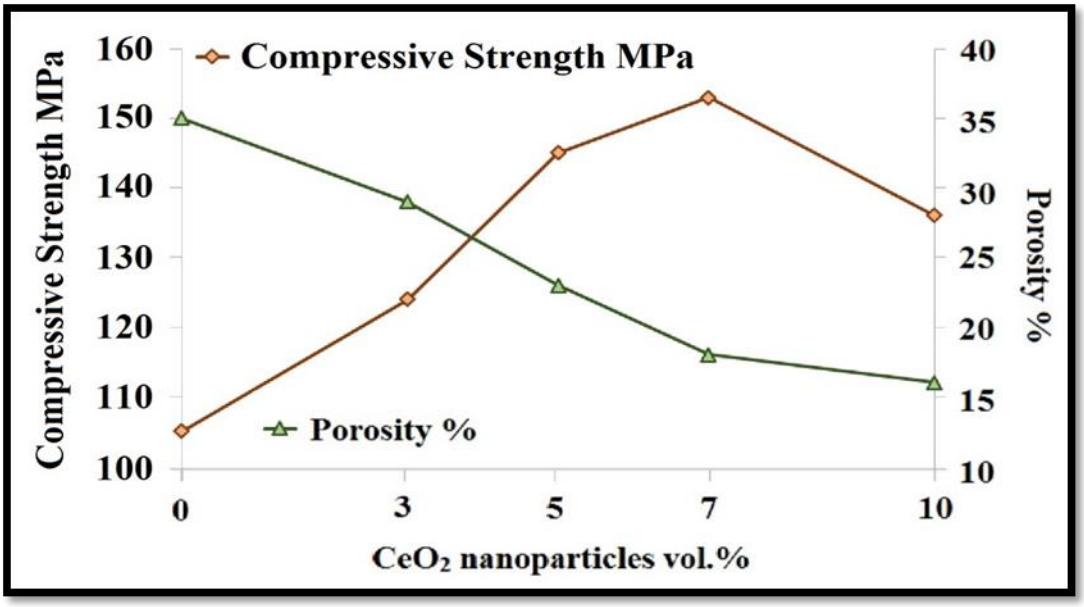

Figure 6: Effect of nanoadditives and porosity percentage on the compressive strength values

Table 1: Alloy samples sets depending on CeO_2 vol.%.

Alloy set No.	Al vol.%	Mg vol.%	CeO_2 vol.%	Ti vol.%
1	15.00	5.00	0	Balance
2	14.55	4.85	3	Balance
3	14.25	4.75	5	Balance
4	13.95	4.65	7	Balance
5	13.5	4.5	10	Balance

5. Conclusion

Practical results showed that increasing the amount of the nanoparticles-additives, have led to a clear increase of micro-hardness and compressive strength values, while there was a decrease in the proportion of porosity was formed. The cause of these results is to create (Ti-CeO2) hard and stable phase, and increased contact between grains of mixture powder points. The best result was at the rate of addition 7 vol.%.

Acknowledgment

The researchers thank the laboratories' personnel of Department of Production and Engineering Metallurgy, for their cooperation and help bring them to accomplish this search.

References

[1] S. Nishikiori, S. Takahashi, S. Satou, T. Tanaka and T. Matsuo, "Microstructure and Creep Strength of Fully-Lamellar Ti3 Al Alloys Containing BetaPhase," Materials Science and Engineering, vol. A329–331, pp. 802–809, 2012.

[2] M. Soboyejo, B. Natarajan, V.K. Vasudevan and D.M. DIMIDUK, "Microstructure Evolution in Gamma Titanium Aluminides Containing Beta-Phase Stabilizers and Boron Addition. Proc. of 2nd Symposium on Structural Intermetallics," edited by M.V. Nathal et al, Seven Springs, PA (USA), September 21-26, pp. 235-244, 2007.

[3] J. Lapin, T. Pelachova, "Microstructural Stability of a Cast Ti-45.2Al-2W-0.6Si-0.7B Alloy at Temperatures 973-1073K," Intermetallics, vol. 14, pp.1175-1180, 2006.

[4] M. Paninski, "Development of a Casting Technology for Complex TiAl Components," Third International Workshop on g-TiAl Technologies, Bamberg, Germany, 29-31 May 2006.

[5] Y. Chen, Y. Chen, F. Kong and S. Xiao, "Fabrication and Processing of Gamma Titanium Aluminides -a Review," Materials Science Forum Vols. 638-642, pp. 1281-1287, 2010.

[6] M. Thomas," Robustness versus Performance Assessment for Different Gamma-TiAl Processing Routes," MRS Boston 2010.

[7] M. Thomas, J-L. Raviart and F. Popoff, "Composition and Microstructural Effects upon Creep Strength of Gas Atomized TiAl Alloy Powder Compacts," Thermec'09, Berlin, 2009.

[8] O. Berteaux, F. Popoff and M. Thomas, "An Experimental Assessment of the Effects of Heat Treatment on the Microstructure of Ti-47Al-2Cr-2Nb Powder

Compacts," Met. Trans. A, vol. 39A, n°10, pp. 2281-2296, 2008.

[9] V. Seetharaman and S.L. Semiatin, "Analysis of Grain Growth in a Two-Phase Gamma Titanium Aluminide Alloy," Metall. Mater. Trans. A, vol. 28A, pp. 947-954, 2013.

[10] Y. Bhambri, V.K. Sikka, W.D. Porter, E.A. Loria and T. Carneiro, "Effect of Composition and Cooling Rate on the Transformation of a to g Phase in TiAl Alloys," Mater. Sci. Eng. A, vol.424, Issues 1-2, pp. 361-365, 2006.

[11] G.X. Guo Fu'an, "Influence de la microstructure sur des propriétésmécaniqueset des contraintes internes d'un alliageintermétalliquebiphasé à base de TiAl," Thèse de doctorat de l'ENSAM Paris, 20 juin 2011.

[12] G.X. Balathandan, L.F. Fu, J.G. Lin, Y.G. Zhang and C.Q. Chen, "The Relationships of Microstructure and Properties of a Fully Lamellar TiAl Alloy. Intermetallics, vol.8, pp. 647-653, 2014.

[13] C.E. NI. Li, K. Yasue, J.G. Lin, Y.G. Zhang and C.Q. Chen, "The Effect of Lamellar Spacing on the Creep Behavior of a Fully Lamellar TiAl Alloy," Intermetallics, vol.8, pp. 525-529, 2013.

[14] G.W. Qin, G.D. W. Smith, B.J. Inkson and R. Dunin-Borkowski, "Distribution Behaviour of Alloying Elements in a2 (a)/g Lamellae of TiAl-Based Alloy," Intermetallics, vol.8, pp. 945-952, 2012.

[15] M. Charpentier, D. Daloz, A. Hazotte and E. Aeby, Gautier, "Toward a Better Understanding of Chemical and Microstructure Heterogeneities Inherited from Solidification and Solid State Phase Transformations in the Ti-48Al-2Cr-2Nb Alloy," Matériaux& Techniques, N°1-2, pp. 39-50, 2014.

[16] T. Novoselova, S. Malinov and W. Sha, "Experimental Study of the Effects of Heat Treatment on Microstructure and Grain Size of a Gamma TiAl Alloy," Intermetallics, vol.11, pp. 491-499, 2013.

[17] R. Yang, "A Theory of the Formation and Growth of Primary Gamma/Alpha2 Lamellae in Fully-Lamellar Gamma-TiAl Based Alloys," International Titanium Aluminide Workshop, Birmingham, UK, 5-7 July 2014.

[18] O. Berteaux, F. Popoff, M. Jouiad, G. Henaff and M. Thomas, "Microstructure Dependence of the Strain Hardening Rate in a PM Ti-48Al-2Cr-2Nb Alloy," Third International Workshop on g-TiAl Technologies, Bamberg, Germany, 29-31 May 2006.

[19] A. Couret, G. Molenat, J. Galy and M. Thomas, "Microstructures and Mechanical Properties of TiAl Alloys Consolidated by Spark Plasma Sintering," Intermetallics, vol. 16 n° 9, pp. 1134-1141, 2008.

[20] Y.L. Hao, D.S. Xu, Y.Y. Cui, R. Yang and D. Li, "The Site Occupancies of Alloying Elements in TiAl and Ti3 Al Alloys," Acta mater. Vol. 47, N° 4, pp. 1129- 1139, 1999.